


**Bulk and shear viscosities in a multicomponent two-dimensional electron system**A. D. Levin,<sup>1</sup> G. M. Gusev<sup>1</sup>, V. A. Chitta<sup>1</sup>, A. S. Jaroshevich<sup>2</sup>, and A. K. Bakarov<sup>2,3</sup><sup>1</sup>*Instituto de Física da Universidade de São Paulo, 135960-170, São Paulo, SP, Brazil*<sup>2</sup>*Institute of Semiconductor Physics, Novosibirsk 630090, Russia*<sup>3</sup>*Novosibirsk State University, Novosibirsk 630090, Russia* (Received 16 August 2024; revised 12 September 2024; accepted 23 October 2024; published 4 November 2024)

We investigated magnetotransport in mesoscopic samples containing electrons from three different subbands in GaAs triple wells. At high temperatures, we observed positive magnetoresistance, which we attribute to the imbalance between different types of particles that are sensitive to bulk viscosities. At low temperatures, we found negative magnetoresistance, attributed to shear viscosity. By analyzing the magnetoresistance data, we were able to determine both viscosities. Remarkably, the electronic bulk viscosity was significantly larger than the shear viscosity. Studying multicomponent electron systems in the hydrodynamic regime presents an intriguing opportunity to further explore the physics in systems with high bulk viscosity.

DOI: [10.1103/PhysRevB.110.195402](https://doi.org/10.1103/PhysRevB.110.195402)**I. INTRODUCTION**

The hydrodynamic description of the fermion-electron system diverges from kinetic theory and presents several intriguing predictions concerning electron transport in small-sized samples, especially in two dimensions. The pivotal concept that significantly advances our understanding of electronic transport phenomena is the notion that, under sufficiently strong electron-electron scattering, an effectively viscous hydrodynamics framework becomes applicable [1–3]. Advances in materials science have enabled systematic investigations using exceptionally clean samples, facilitating the observation of a wide range of hydrodynamic effects.

These effects encompass resistance reduction with temperature (known as the Gurzhi effect) [1,2,4–7], giant negative magnetoresistance [3,5,8–14], negative nonlocal resistance [15–18], superballistic flow [19,20], hydrodynamics with obstacles [21–24], photogenerated electron hole plasma [25,26], and modifications to the Hall effect [27–32]. The recent progress overview in electronic hydrodynamics has been presented in the papers [33] and [34].

In narrow channels, electron flow resembles Poiseuille flow of liquid in a pipe, where velocities near the walls approach zero. It has been established that the resistivity of a narrow strip follows the formula [1]  $\rho = \frac{m}{ne^2} \eta \frac{12}{W^2}$ , where  $m$  denotes the effective mass,  $n$  represents the density,  $W$  signifies the strip width, and  $\eta$  stands for shear viscosity; the shear viscosity can be derived using the Kubo formula [35]. For a two-dimensional system, it is given by  $\eta = \frac{1}{4} v_F^2 \tau_{2,ee}$ , where  $v_F$  denotes the Fermi velocity and  $\tau_{2,ee}$  represents the shear stress relaxation time due to electron-electron scattering, with the subscript “2” indicating that the viscosity coefficient is determined by the relaxation of the second harmonic of the distribution function [10].

References [7,29,36] provide a coherent microscopic calculation of bulk viscosity for two-dimensional electrons in a sample featuring defects of small radius. The bulk or second viscosity, denoted as  $\zeta$ , characterizes the dissipation

that occurs within a liquid when it experiences a uniform compressionlike deformation. It has remained one of the controversial subjects of fluid dynamics [37]. Understanding the volume viscosity is crucial for grasping various fluid phenomena, such as sound attenuation in multiatomic gases and the propagation of shock waves [37]. However, in a monatomic gas at low density and in an electron Fermi liquid, volume viscosity is zero [38]. Nevertheless, some common fluids exhibit bulk viscosities that are hundreds to thousands of times greater than their shear viscosities [39]. Deriving bulk viscosity experimentally is complex. To study bulk viscosity in Fermi liquid, several challenges must be addressed. First, it is essential to identify a system where the bulk viscosity is significantly enhanced and measurable. Second, it is necessary to determine how this effect can be easily extracted experimentally. Multicomponent systems offer a useful platform for exploring bulk viscosity.

Recent demonstrations have highlighted the significant role of bulk viscosity in the viscous flow of a two-component electron fluid [40]. Positive saturating magnetoresistance has been predicted for a two-component electron fluid in narrow samples. For example, in a double quantum well, intersubband scattering, which transforms one type of particle into another, can lead to an imbalance in flow depending on the bulk viscosity. The magnetic field induces a transition from regimes of independent flows of the two fluid components to a regime where imbalance occurs near the edge regions [40]. It is worth noting that the theory for a two-component system can be readily extended to triple and multicomponent electron systems.

Previous studies have explored hydrodynamic transport in two-component electron-hole systems within compensated semimetals [41]. It has been shown that recombination effects near the edge are crucial, contributing to linear positive magnetoresistance. The interaction between shear viscosity and recombination effects in mesoscopic compensated semimetals has been explored in [42], but the impact of bulk viscosity was not examined.

In this study, we employed a triple-well system with high barrier heights. Transport measurements in this system reveal significantly different scattering times between the central well and the lateral wells. Electrons in the central well experience rare transitions to the lateral wells during scattering events, which is a necessary condition for the model proposed in [40]. We compared these results with those from a triple-well system with low barriers, where the scattering times are nearly equal across all wells, and we did not observe positive magnetoresistance induced by bulk viscosity. This is because the conditions of the theory are not met, as the transport properties in different subbands are not significantly different. Additionally, in our previous studies [6], we did not observe positive magnetoresistance in a double-well system, as the necessary conditions were not fully met. By comparing the theoretical predictions from [40] with the observed positive magnetoresistance at high temperature, we were able to derive the bulk viscosity. Notably, the bulk viscosity was found to be much larger than the shear viscosity.

Additionally, we investigate negative magnetoresistance at lower temperature resulting from the magnetic field's influence on shear viscosity. We also determine the characteristic shear stress relaxation time of electrons, which is influenced by electron-electron scattering.

## II. EXPERIMENTAL RESULTS AND DISCUSSION

Our samples consist of symmetrically doped GaAs triple quantum wells (TQWs), separated by  $\text{Al}_x\text{Ga}_{1-x}\text{As}$  and AlAs barriers. They feature a high total electron sheet density of  $n_s \approx 9 \times 10^{11} \text{cm}^{-2}$  and mobilities of  $4.5 \times 10^5 \text{cm}^2/\text{Vs}$ . The central well is approximately  $220 \text{ \AA}$  wide, with both side wells having equal widths of  $100 \text{ \AA}$ . The barrier thickness  $d_b$  is  $20 \text{ \AA}$  for AlAs (wafer A) and for AlGaAs (wafer B).

The transport properties of these triple wells have been extensively investigated, encompassing phenomena such as magnetointersubband oscillations in low magnetic fields, microwave-induced oscillations, and the fractional quantum Hall effect [43–45]. Detailed parameters of the quantum wells, including mobility, density, and structural characteristics, can be found in the Supplemental Material [46]. The average mean free path in macroscopic samples approaches  $l = (6 - 3.8) \mu\text{m}$ , which exceeds the sample width  $W$  [46]. Hence, the hydrodynamic condition  $W < l$  is satisfied. The mesoscopic sample is a Hall bar device featuring two current probes and seven voltage probes. The bar has a width  $W$  of  $3.2 \mu\text{m}$ , and consists of three consecutive segments with different lengths,  $L$ , of  $2.8 \mu\text{m}$ ,  $8.6 \mu\text{m}$ , and  $32 \mu\text{m}$ . Details of the sample geometry, configuration, and measurement techniques are provided in [46]. Measurements were conducted on two samples of each type of wafer (A and B), i.e., in four samples. We present the results for two samples, as the results for the other two samples are identical.

Figure 1(a) depicts the evolution of resistance with magnetic field at various temperatures for sample A, which was fabricated using TQW with AlAs barriers. To improve hydrodynamic characteristics, current was applied between side probes, while voltage was measured across opposite side probes, utilizing an H-type geometry as described in [5,46].

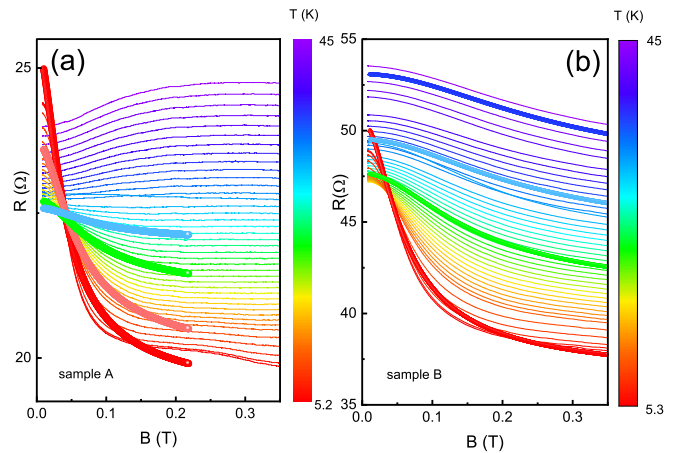


FIG. 1. (a) Temperature-dependent magnetoresistivity of triple quantum wells (sample A). The circles (thick lines) are examples illustrating magnetoresistance calculated from Eq. (1) for different temperatures  $T$  (K): 5.3 (red), 11 (orange), 21 (green), and 27 (cyan). (b) Temperature-dependent magnetoresistivity of triple quantum wells (sample B). The circles (thick lines) are examples illustrating magnetoresistance calculated from Eq. (1) for different temperatures  $T$  (K): 5.3 (red), 23 (green), 35 (cyan), and 44 (blue).

It is noteworthy that the large negative magnetoresistance, characterized by a Lorentzian profile [i.e.,  $R(B) - R(0) < 0$ ], diminishes in magnitude and broadens as temperature rises. Furthermore, the resistivity at zero magnetic field exhibits a decrease with temperature within the range of  $5 \text{ K} < T < 25 \text{ K}$  (known as the Gurzhi effect), followed by a subsequent increase. This observation aligns with earlier findings interpreted as distinct hallmarks of hydrodynamic behavior [5]. Figure 1(b) illustrates the pronounced negative magnetoresistance observed in sample B with  $\text{Al}_x\text{Ga}_{1-x}\text{As}$  barriers. It is noteworthy that the behavior of Sample A contrasts distinctly with that of Sample B: above  $25 \text{ K}$ , the negative magnetoresistance diminishes and is replaced by significant positive magnetoresistance, saturating above  $0.2 \text{ T}$ . The resistance at zero field for sample A is found to be two times smaller than that of sample B, despite the fact that all macroscopic characteristics of the samples are almost identical. We attribute the negative magnetoresistance in both samples at low temperatures to hydrodynamic effects arising from shear electron viscosity. Conversely, the positive magnetoresistance for sample A at high temperatures is attributed to transverse current imbalance governed by bulk viscosity, in accordance with predictions [40].

To qualitatively compare with experimental data, we utilize a model proposed in previous studies, originally developed for Poiseuille flow in the presence of a magnetic field in a single conductive layer [8,40]. We have adapted this model for our specific configuration, which includes a common contact across all three layers. Resistance can be expressed in the form  $R = \frac{L}{W} \rho_{\text{total}} = (\rho_1^{-1} + \rho_2^{-1} + \rho_3^{-1})^{-1}$ , and  $\rho_i$  is given by the equation below. In its simplified form, the model characterizes resistivity through two distinct contributions. The first arises from ballistic effects or scattering at boundaries and defects, while the second is controlled by viscosity [8]. In a more

TABLE I. Fitting parameters of the electron system for different configurations. Parameters are defined in the text.

Sample	$1/\tau_{2,\text{imp}}$ ( $10^{11}$ 1/s)	$1/\tau_{0,\text{imp}}$ ( $10^{10}$ 1/s)	$B_{ph}$ ( $10^9$ 1/sK)	$W^*$ $\mu\text{m}$
A	1.1	2	1	7.5
B	2.1	3.0	1.3	3.5

comprehensive formulation, the theory involves employing a viscosity tensor that depends on the magnetic field in order to derive the resistivity tensor for the  $i$ th subband:

$$\rho_i(B) = \left( \frac{m}{e^2 n_i} \right) \frac{1}{1 - \tanh(\xi_i)/\xi_i}. \quad (1)$$

Here, the dimensionless Gurzhi parameter  $\xi = \xi_0 \sqrt{1 + (2l_2/r_c)^2}$ ,  $\xi_0 = W^*/l_G$ , where  $l_G = \sqrt{l_2 l}$  is the Gurzhi length;  $l_2 = v_F \tau_2$ ,  $l = v_F \tau$ ,  $r_c = v_F/\omega_c$  is the cyclotron radius;  $\omega_c = eB/mc$  represents the cyclotron frequency; and  $W^*$  is the effective sample width. The relaxation rate for shear viscosity is given by  $1/\tau_2(T) = 1/\tau_{2,ee}(T) + 1/\tau_{2,\text{imp}}$ . The momentum relaxation rate is expressed as  $1/\tau(T) = 1/\tau_{0,ph}(T) + 1/\tau_{0,\text{imp}}$ , where  $1/\tau_{0,ph} = B_{ph}T$  represents the term associated with phonon scattering, and  $1/\tau_{0,\text{imp}}$  denotes the scattering time due to static disorder (not related to the relaxation time of the second moment) [8,10]. Next, we fit the magnetoresistance curves and the resistivity  $R(T)$  at zero magnetic field shown in Fig 1. For simplicity, the fitting procedure employs three parameters:  $\tau(T)$ ,  $\tau_2(T)$ , and the width of the sample  $W$ . In this case, we propose that the shear scattering time is nearly identical for different subbands; otherwise, fitting with numerous parameters would become excessively ambiguous. We observe excellent agreement with Eq. (1) across a broad range of magnetic fields and temperatures for sample B. However, the fitting of the data for sample A is somewhat poorer, suggesting that additional mechanisms governing hydrodynamic properties may need to be considered. The parameters extracted from comparing the relaxation rates and theoretical equations are presented in Table I.

The total inelastic scattering rate arises from both inter-subband transitions and intrasubband processes, expressed as  $(1/\tau_{ee})^{\text{tot},i} = (1/\tau_{ee})^{\text{inter},i} + (1/\tau_{ee})^{\text{intra},i}$ , where  $i=1,2,3$  denotes the subband number. Electron-electron scattering is anticipated to be more intense due to enhanced screening effectiveness and a tripling of the phase space for intrasubband rates compared to the single-band scenario [47]. The inelastic scattering rate for the intrasubband processes is given by  $(\hbar/\tau_{ee})^{\text{intra},i} = -A_1(kT)^2/E_F + A_2[(kT)^2/E_F][\ln(4E_F/kT)]$ . And for intersubband scattering,  $(\hbar/\tau_{ee})^{\text{inter},i} = -B_1(kT)^2/E_F + B_2[(kT)^2/E_F][\ln(4E_F/\Delta) + B_3[(kT)^2/E_F][\ln(\Delta/kT)]$ . Everywhere,  $A_j$  and  $B_j$  are positive numerical constants of order unity. The relaxation rate  $1/\tau_{2,\text{imp}}(T)$ , arising from processes relaxing the second harmonic of the distribution function, includes scattering by static defects contributing to viscosity. Conversely,  $1/\tau_{2,ee}(T)$  corresponds to the relaxation of shear viscosity due to electron-electron scattering [8,10]. Figure 2(a) demonstrates the temperature dependence of the relaxation rate  $1/\tau_{2,ee}(T)$

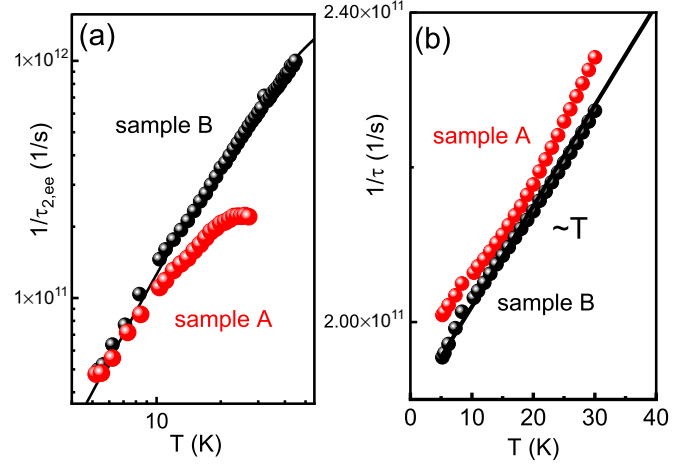


FIG. 2. (a) Relaxation rate  $1/\tau_{2,ee}$  as a function of temperature obtained by fitting the theory with experimental results for sample A (red circles) and sample B (black circles). Black line theory. (b) Relaxation rate  $1/\tau$  as a function of temperature obtained by fitting the theory with experimental data.

for both samples. For comparison with theory, we simplified the situation by assuming equal parameters for each subband and  $1/\tau_{2,ee}(T) \approx 1/\tau_{ee}(T)$ . The solid line represents the theoretical comparison with parameters. Figure 1(a) shows the theoretical predictions with parameters  $A_1 = B_1 = 0.35$  and  $A_2 = B_2 = B_3 = 0.26$ . In sample A, we observe deviations in the scattering rate at high temperatures, suggesting that additional mechanisms are influencing the hydrodynamic flow in this sample.

We obtain  $1/\tau_1 \approx 1/\tau_2 \approx 1/\tau_3 \approx 1/\tau$  for sample B and  $1/\tau_1 \approx 1/\tau_2 \approx 1/\tau$ ,  $1/\tau_3 \approx 1/3\tau$  for sample A. Note that this ratio can vary and does not affect the shear relaxation time, which depends on the shape of the magnetoresistance. However, for other ratios, we obtain a coefficient  $B_{ph}$  responsible for electron-phonon scattering, much higher than the value of  $1 \times 10^9$  1/sK. For example, if we assume that all subbands in sample A have a similar  $1/\tau$  (as we proposed for sample B), the coefficient  $B_{ph}$  is half the value reported in the literature or what we found in sample B. It is natural to assume that the penetration through the barriers depends exponentially on the height of the barrier. In the sample with low barriers, the wave functions for all subbands are spread across all three wells, so the scattering rate is expected to be nearly equal for all subbands. However, in sample A, with AlAs barriers, the wave functions are mostly localized in either the central or lateral wells, leading to different scattering rates. It demonstrates that electrons from different subbands in sample A exhibit nearly independent dynamics, with infrequent transformations into each other during scattering events. This characteristic is a necessary requirement for the model proposed in [40], which predicts hydrodynamic-induced positive magnetoresistance at high temperatures, as discussed below. Figure 2(b) illustrates the dependence of the rate  $1/\tau$  on temperature. It shows a linear trend, consistent with theoretical expectations. The value of  $B_{ph}$  agrees with previously calculated parameters that characterize the electron-phonon coupling in GaAs systems [5,18].

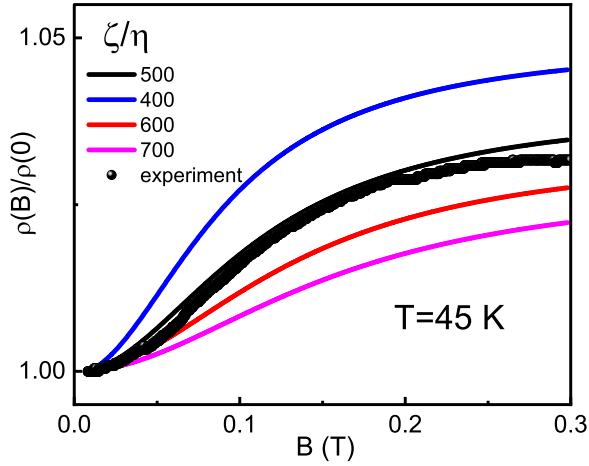


FIG. 3. Dependence of the relative sample resistivity  $\rho(B)/\rho(0)$  on magnetic field  $B$  for several values of bulk viscosity  $\zeta$  (black circles),  $T = 45$  K (sample A). Solid line theoretical magnetoresistance calculated for different ratios of  $\zeta/\eta$ .

It is noteworthy that we also derive the effective sample width  $W^*$  and obtain reasonable agreement for sample B:  $W^* \approx 3.5$   $\mu\text{m}$ , which is slightly higher than geometric width  $W \approx 3$   $\mu\text{m}$ . However, we observe a significantly different value for sample A (see Table I), which further suggests that additional mechanisms are influencing the hydrodynamic flow in this sample.

To describe the positive magnetoresistivity at high temperatures for sample A [Fig. 1(b)], we utilize the model proposed in [40]. This model examines a two-component electron liquid, where electron scattering and transitions between components can induce imbalances in flows and concentrations. This imbalance is particularly sensitive to bulk viscosity. Under the influence of a magnetic field, the system transitions from independent, uniform Ohmic flows of two carrier types to flows involving recombinations of these carriers, resulting in positive magnetoresistance. Note that the magnetic dependence of shear viscosity in this case is weak and negligible, as observed at elevated temperatures  $T > 45$  K, where the shear relaxation rate is high. For a pure hydrodynamic case, the conductivity in the presence of the magnetic field is given by

$$\begin{aligned} \sigma_{hydr}(T, B) &= \frac{e^2 n_{tot}}{m^*} \frac{1}{\left(\frac{n_1^*}{n_{tot}} \eta_1 + \frac{n_2}{n_{tot}} \eta_2\right)} \\ &\times \left\{ \frac{W^2}{12} + \frac{2\zeta\lambda}{\omega_c^2} \frac{n_1^* n_2 (\eta_1 - \eta_2)^2}{n_{tot} (n_1^* \eta_1 + n_2 \eta_2)} \right. \\ &\left. \times \Re e \left[ \sqrt{i} \tanh \left( \sqrt{i} \frac{\lambda W}{2} \right) \right] \right\}. \end{aligned} \quad (2)$$

Here,  $\lambda = \sqrt{\omega_c} \sqrt{\frac{a_s}{\zeta \eta}}$ , where  $1/\lambda$  represents the characteristic length that defines the widths of the near-edge regions,  $\eta = \eta_1 + \eta_2$ . These regions are crucial for intense diffusion and particle type transformations, which in turn define the bulk viscosity  $\zeta$  and facilitate the diffuse transport of momentum  $x$  components in the  $y$  direction perpendicular to the channel due to shear viscosity effects in the fluid. The density  $n_{tot}$  is

the total carrier concentration,  $\omega_c = eB/mc$  is the cyclotron frequency, and  $n_i$  and  $\eta_i$  are corresponding density and viscosity of  $i$ th subbands. For simplicity, we propose that both lateral wells have similar density and viscosity, thus  $n_1^* = 2n_1$  and  $\eta_1 \approx \eta_3 = \frac{1}{4} v_{F,1}^2 \tau_{2,ee}$ ,  $\eta_2 = \frac{1}{4} v_{F,2}^2 \tau_{2,ee}$ , where  $v_{F,i}$  denotes the Fermi velocity dependent on density, while  $\tau_{2,ee}$  remains independent of the subband index. At low magnetic field, Eq. (3) can be expressed as  $\sigma_{hydr}(T, 0) = \frac{e^2 W^2}{m} \left( \frac{n_1^*}{\eta_1} + \frac{n_2}{\eta_2} \right)$ . This equation describes the Poiseuille flow of a uniform two-component fluid, incorporating contributions from both components' shear viscosities. In a strong magnetic field, Eq. (3) transforms to  $\sigma_{hydr}(T, \infty) = \frac{e^2 n_{tot}}{m^*} \frac{1}{\left(\frac{n_1^*}{n_{tot}} \eta_1 + \frac{n_2}{n_{tot}} \eta_2\right)} \frac{W^2}{12}$ . This value corresponds to the sum of two independent Poiseuille flows involving different types of particles. The transition between these regimes corresponding to positive magnetoresistance (negative magnetoconductance) is a smooth crossover that occurs at magnetic field  $B^* = mc\omega^*/e$  with the characteristic borderline cyclotron frequency,  $\omega^* = \sqrt{\frac{\zeta \eta}{a_s}} \frac{1}{W^2}$ , where  $a_s = \frac{\eta}{n_{tot}} \left( \frac{n_2}{\eta_1} + \frac{n_1^*}{\eta_2} \right)$ . We expressed the total conductivity in the form  $\sigma_{total} = \sum_{i=1}^3 e^2 n_i \tau_i / m + \sigma_{hydr}$ . Figure 3 shows a comparison of the relative magnetoresistivity with the theoretical model [40], using parameters derived from the analysis of the negative magnetoresistance described in the previous sections (Fig. 1). We approximate the temperature dependence of relaxation times  $\tau_{2,ee}$  and  $\tau$  at high temperatures, using viscosity  $\zeta$  as a fitting parameter. We find good agreement for the ratio  $\zeta/\eta = 500$ , corresponding to  $\zeta \approx 17$   $\text{m}^2/\text{s}$ . Additionally, we determine  $\eta_1 = 0.026$   $\text{m}^2/\text{s}$  and  $\eta_2 = 0.0134$   $\text{m}^2/\text{s}$ . These shear viscosity values are consistent with those previously reported for similar temperatures [5,18]. It is well known that the Boltzmann kinetic equation predicts a zero value for bulk viscosity in a monatomic gas [38]. Estimating bulk viscosity in interacting Fermi gases has been addressed [48], but extracting it from experiments remains an experimental challenge [37]. In multicomponent molecular liquids, a significant bulk viscosity arises due to relatively slow, reversible chemical reactions between the liquid's components [39].

### III. CONCLUSION

In conclusion, we investigated hydrodynamic magnetotransport in triple quantum wells. In addition to observing negative magnetoresistance, we also noted positive magnetoresistance, attributed to an imbalance near the edges and governed by bulk viscosity. Both bulk and shear viscosities were deduced from our analysis of these magnetoresistances. Studying magnetoresistance in multicomponent systems paves the way for investigating large bulk viscosity, a parameter challenging to determine through other experiments.

### ACKNOWLEDGMENTS

We thank P.S. Alekseev for helpful discussions. This work is supported by FAPESP (São Paulo Research Foundation) Grants No. 2019/16736-2, No. 2021/12470-8, No. 2024/06755-8, and CNPq (National Council for Scientific and Technological Development).



- [1] R. N. Gurzhi, Minimum of resistance in impurity-free conductors, *Sov. Phys. JETP* **44**, 771 (1963) ; Reviews of topical problems: Hydrodynamic effects in solids at low temperature, *Sov. Phys. Usp.* **11**, 255 (1968).
- [2] A. V. Andreev, S. A. Kivelson, and B. Spivak, Hydrodynamic description of transport in strongly correlated electron systems, *Phys. Rev. Lett.* **106**, 256804 (2011).
- [3] B. N. Narozhny, I. V. Gornyi, M. Titov, M. Schutt, and A. D. Mirlin, Hydrodynamics in graphene: Linear-response transport, *Phys. Rev. B* **91**, 035414 (2015).
- [4] M. J. M. de Jong and L. W. Molenkamp, Hydrodynamic electron flow in high-mobility wires, *Phys. Rev. B* **51**, 13389 (1995).
- [5] G. M. Gusev, A. D. Levin, E. V. Levinson, and A. K. Bakarov, Viscous electron flow in mesoscopic two-dimensional electron gas, *AIP Adv.* **8**, 025318 (2018).
- [6] G. M. Gusev, A. S. Yaroshevich, A. D. Levin, Z. D. Kvon and A. K. Bakarov, Viscous magnetotransport and Gurzhi effect in bilayer electron system, *Phys. Rev. B* **103**, 075303 (2021).
- [7] A. Principi, G. Vignale, M. Carrega, and M. Polini, Bulk and shear viscosities of the two-dimensional electron liquid in a doped graphene sheet, *Phys. Rev. B* **93**, 125410 (2016).
- [8] P. S. Alekseev, Negative magnetoresistance in viscous flow of two-dimensional electrons, *Phys. Rev. Lett.* **117**, 166601 (2016).
- [9] B. N. Narozhny and M. Schutt, Magnetohydrodynamics in graphene: Shear and Hall viscosities, *Phys. Rev. B* **100**, 035125 (2019).
- [10] P. S. Alekseev and A. P. Dmitriev, Viscosity of two-dimensional electrons, *Phys. Rev. B* **102**, 241409(R) (2020).
- [11] O. E. Raichev, G. M. Gusev, A. D. Levin, and A. K. Bakarov, Manifestations of classical size effect and electronic viscosity in the magnetoresistance of narrow two-dimensional conductors: Theory and experiment, *Phys. Rev. B* **101**, 235314 (2020).
- [12] D. A. Khudaiberdiev, G. M. Gusev, E. B. Olshanetsky, Z. D. Kvon, and N. N. Mikhailov, Magnetohydrodynamics and electron-electron interaction of massless Dirac fermions, *Phys. Rev. Res.* **3**, L032031 (2021).
- [13] X. Wang, P. Jia, R.-R. Du, L. N. Pfeiffer, K. W. Baldwin, and K. W. West, Hydrodynamic charge transport in an GaAs/AlGaAs ultrahigh-mobility two-dimensional electron gas, *Phys. Rev. B* **106**, L241302 (2022).
- [14] A. D. Levin, G. M. Gusev, A. S. Yaroshevich, Z. D. Kvon, and A. K. Bakarov, Geometric engineering of viscous magnetotransport in a two-dimensional electron system, *Phys. Rev. B* **108**, 115310 (2023).
- [15] D. A. Bandurin, I. Torre, R. Krishna Kumar, M. Ben Shalom, A. Tomadin, A. Principi, G. H. Auton, E. Khestanova, K. S. Novoselov, I. V. Grigorieva, L. A. Ponomarenko, A. K. Geim, and M. Polini, Negative local resistance caused by viscous electron backflow in graphene, *Science* **351**, 1055 (2016).
- [16] I. Torre, A. Tomadin, A. K. Geim, and M. Polini, Nonlocal transport and the hydrodynamic shear viscosity in graphene, *Phys. Rev. B* **92**, 165433 (2015).
- [17] F. M. D. Pellegrino, I. Torre, and M. Polini, Nonlocal transport and the Hall viscosity of two-dimensional hydrodynamic electron liquids, *Phys. Rev. B* **96**, 195401 (2017).
- [18] A. D. Levin, G. M. Gusev, E. V. Levinson, Z. D. Kvon, and A. K. Bakarov, Vorticity-induced negative nonlocal resistance in a viscous two-dimensional electron system, *Phys. Rev. B* **97**, 245308 (2018).
- [19] R. Krishna Kumar, D. A. Bandurin, F. M. D. Pellegrino, Y. Cao, A. Principi, H. Guo, G. H. Auton, M. Ben Shalom, L. A. Ponomarenko, G. Falkovich, K. Watanabe, T. Taniguchi, I. V. Grigorieva, L. S. Levitov, M. Polini, and A. K. Geim, Superballistic flow of viscous electron fluid through graphene constrictions, *Nat. Phys.* **13**, 1182 (2017).
- [20] T. Holder, R. Queiroz, T. Scaffidi, N. Silberstein, A. Rozen, J. A. Sulpizio, L. Ella, S. Ilani, and A. Stern, Ballistic and hydrodynamic magnetotransport in narrow channels, *Phys. Rev. B* **100**, 245305 (2019).
- [21] A. Lucas, Stokes paradox in electronic Fermi liquids, *Phys. Rev. B* **95**, 115425 (2017).
- [22] G. M. Gusev, A. S. Yaroshevich, A. D. Levin, Z. D. Kvon, and A. K. Bakarov, Stokes flow around an obstacle in viscous two-dimensional electron liquid, *Sci. Rep.* **10**, 7860 (2020).
- [23] I. V. Gornyi and D. G. Polyakov, Two-dimensional electron hydrodynamics in a random array of impenetrable obstacles: Magnetoresistivity, Hall viscosity, and the Landauer dipole, *Phys. Rev. B* **108**, 165429 (2023).
- [24] Zachary J. Krebs, Wyatt A. Behn, Songci Li, Keenan J. Smith, Kenji Watanabe, Takashi Taniguchi, Alex Levchenko, Victor W. Brar, Imaging the breaking of electrostatic dams in graphene for ballistic and viscous fluids, *Science* **379**, 671 (2023).
- [25] Y. A. Pusep, M. D. Teodoro, V. Laurindo Jr., E. R. Cardozo de Oliveira, G. M. Gusev, and A. K. Bakarov, Diffusion of photoexcited holes in a viscous electron fluid, *Phys. Rev. Lett.* **128**, 136801 (2022).
- [26] M. A. T. Patricio, G. M. Jacobsen, M. D. Teodoro, G. M. Gusev, A. K. Bakarov, and Y. A. Pusep, Hydrodynamics of electron-hole fluid photogenerated in a mesoscopic two-dimensional channel, *Phys. Rev. B* **109**, L121401 (2024).
- [27] A. I. Berdyugin, S. G. Xu, F. M. D. Pellegrino, R. Krishna Kumar, A. Principi, I. Torre, M. Ben Shalom, T. Taniguchi, K. Watanabe, I. V. Grigorieva, M. Polini, A. K. Geim, and D. A. Bandurin, Measuring Hall viscosity of graphene's electron fluid, *Science* **364**, 162 (2019).
- [28] T. Scaffidi, N. Nandi, B. Schmidt, A. P. Mackenzie, and J. E. Moore, Hydrodynamic electron flow and Hall viscosity, *Phys. Rev. Lett.* **118**, 226601 (2017).
- [29] I. S. Burmistrov, M. Goldstein, M. Kot, V. D. Kurilovich, and P. D. Kurilovich, Dissipative and Hall viscosity of a disordered 2D electron gas, *Phys. Rev. Lett.* **123**, 026804 (2019).
- [30] P. S. Alekseev and M. A. Semina, Ballistic flow of two-dimensional interacting electrons, *Phys. Rev. B* **98**, 165412 (2018).
- [31] P. S. Alekseev and M. A. Semina, Hall effect in a ballistic flow of two-dimensional interacting particles, *Phys. Rev. B* **100**, 125419 (2019).
- [32] G. M. Gusev, A. D. Levin, E. V. Levinson, and A. K. Bakarov, Viscous transport and Hall viscosity in a two-dimensional electron system, *Phys. Rev. B* **98**, 161303(R) (2018).
- [33] M. Polini, and A. K. Geim, Viscous electron fluids, *Phys. Today* **73**(6), 28 (2020).
- [34] B. N. Narozhny, Hydrodynamic approach to two-dimensional electron systems, *La Rivista del Nuovo Cimento* **45**, 661 (2022).
- [35] B. Bradlyn, M. Goldstein, and N. Read, Kubo formulas for viscosity: Hall viscosity, Ward identities, and the relation with conductivity, *Phys. Rev. B* **86**, 245309 (2012).

- [36] V. A. Zakharov and I. S. Burmistrov, Residual bulk viscosity of a disordered two-dimensional electron gas, *Phys. Rev. B* **103**, 235305 (2021).
- [37] B. Sharma, R. Kumar, A brief introduction to bulk viscosity of fluids, physics [arXiv:2303.08400](https://arxiv.org/abs/2303.08400).
- [38] I. Khalatnikov, The second viscosity of monoatomic gases, *Sov. Phys. JETP* **2**, 169 (1955).
- [39] M. S. Cramer, Numerical estimates for the bulk viscosity of ideal gases, *Phys. Fluids* **24**, 066102 (2012).
- [40] P. S. Alekseev, Viscous flow of two-component electron fluid in magnetic field, *Semiconductors* **57**, 193 (2023).
- [41] P. S. Alekseev, A. P. Dmitriev, I. V. Gornyi, V. Yu. Kachorovskii, B. N. Narozhny, M. Schutt, and M. Titov, Magnetoresistance in two-component systems, *Phys. Rev. Lett.* **114**, 156601 (2015).
- [42] P. S. Alekseev, A. P. Dmitriev, I. V. Gornyi, V. Yu. Kachorovskii, B. N. Narozhny, M. Schutt, and M. Titov, Magnetoresistance of compensated semimetals in confined geometries, *Phys. Rev. B* **95**, 165410 (2017).
- [43] S. Wiedmann, N. C. Mamani, G. M. Gusev, O. E. Raichev, A. K. Bakarov, and J. C. Portal, Magnetoresistance oscillations in multilayer systems: Triple wells, *Phys. Rev. B* **80**, 245306 (2009).
- [44] S. Wiedmann, N. C. Mamani, G. M. Gusev, O. E. Raichev, A. K. Bakarov, and J. C. Portal, Magneto-intersubband oscillations in triple quantum wells, *Physica E* **42**, 1088 (2010).
- [45] G. M. Gusev, S. Wiedmann, O. E. Raichev, A. K. Bakarov, and J. C. Portal, Emergent and reentrant fractional quantum Hall effect in trilayer systems in a tilted magnetic field, *Phys. Rev. B* **80**, 161302(R) (2009).
- [46] See Supplemental Material at <http://link.aps.org/supplemental/10.1103/PhysRevB.110.195402> for details of the triple quantum well and transport analyses, which also contains Refs. [10,43–45].
- [47] M. Slutzky, O. Entin-Wohlman, Y. Berk, A. Palevski, and H. Shtrikman, Electron-electron scattering in coupled quantum wells, *Phys. Rev. B* **53**, 4065 (1996).
- [48] M. Holten, L. Bayha, A. C. Klein, P. A. Murthy, P. M. Preiss, and S. Jochim, Anomalous breaking of scale invariance in a two-dimensional Fermi gas, *Phys. Rev. Lett.* **121**, 120401 (2018).